

MODELING DISTORTION OF SUPER-WIDE-ANGLE LENSES FOR ARCHITECTURAL AND ARCHAEOLOGICAL APPLICATIONS

G. E. Karras, G. Mountrakis, P. Patias*, E. Petsa**

Department of Surveying, National Technical University, GR-15780 Athens, Greece (gkarras@central.ntua.gr)

*Department of Cadastre, Photogrammetry & Cartography, The Aristotle University, GR-54006 Thessaloniki, Greece

**Department of Surveying, Technological Educational Institute, GR-12210 Athens, Greece

Commission V, Working Group 5

KEY WORDS: Lens Distortion, Super-Wide-Angle Lenses, Architectural Photogrammetry, Resampling

ABSTRACT

Mapping of architectural and archaeological objects often encounters limitations in imaging distances (interiors, narrow streets, excavations), usually tackled via large numbers of images or special camera platforms. This, however, seriously contradicts the benefits of simple, low-cost photogrammetric procedures. In these cases, furthermore, the use of digital cameras with the currently limited area of sensitive sensors may also be impracticable. In this context, the employment of super-wide-angle lenses (e. g. of 14, 17 or 18 mm focal lengths for 35 mm cameras) appears as a possible remedy; these, however, suffer from heavy distortions. This paper presents a first study of two different 17 mm lenses commonly available in the market (RMC Tokina and SP Tamron on Nikon cameras). In order to assess their photogrammetric potential, the efficiency of the conventional model for radial symmetric lens distortion has been tested. Partial calibration was performed using photography of straight lines easily found in urban environments. Overall precisions of line fitting, initially 4.2 and 6.3 pixels, rose after correcting distortion to 1.3 and 1.5 pixels, respectively; thus, the main cause of deviations seems to have been removed. Repeatability of calibration, on the other hand, is also regarded as satisfactory (presence of decentering distortion was difficult to establish). Digital image transformation, also performed here, results in resampled imagery essentially freed from lens distortion and suitable for common digital photogrammetric software.

1. INTRODUCTION

Everyone involved in the photogrammetric documentation of objects of architectural and archaeological interest has probably wished, at one time or another, that the camera had a shorter focal length. Indeed, in this field one often encounters strict limitations in imaging distance, as is the case with interiors (in churches, tombs, corridors, passages) and confined spaces, photography in narrow streets or with recording objects stretching horizontally, exemplified in the documentation of the progress of excavations. Such situations may either lead to excessive numbers of images or (as in the case of excavations) require special camera platforms.

Of course, super-wide angle photography with metric cameras, notably the Wild P31, is also an answer to several of these problems. In certain instances, fish-eye imagery can also be considered (e.g. Boulianne et al., 1997); however, this is not directly suitable for simple documentation purposes and implies a somewhat elaborate treatment. In routine tasks of medium and low accuracy requirements, all above solutions contradict the benefits – so often promised – of simple, low-cost photogrammetric procedures with amateur cameras.

In this context, a basic remedy seems to be the employment of super-wide-angle lenses, e. g. of 14, 17 or 18 mm focal lengths, with 35 mm cameras. Several such lenses are widely available at low prices and (unlike the fish-eye lens) produce “ordinary” photographs. Of course, a larger angular field of view ($>100^\circ$) is followed by smaller scales; rapid variation of scale within the image; strong displacements due to relief and, consequently, occlusion of object areas. In this sense, it is by no means to be viewed as a panacea; its use is a question of practical considerations. However, the wide-angle lens is useful for documentation

purposes as illustrated in Fig. 1 (vertical photograph of an excavation: $H = 3.4$ m; $f = 17$ mm; negative scale 1:200; camera simply fixed at the top of a leveling staff).



Figure 1. Photograph of an excavation with a 17 mm lens.

It is more important, of course, that such a lens may well be used in a variety of purely metric tasks (rectification of surfaces of small relief being the simplest among them). However, their photogrammetric use inevitably raises the crucial question of lens distortion.

Indeed, these lenses usually suffer from heavy distortions which need to be assessed and modeled if their photogrammetric potential is to be exploited. Radial symmetric distortion – whose effects immediately strike the observer of enlarged prints – is anticipated as the main problem. The efficiency of the conventional lens distortion model in grasping and correcting these effects has to be checked. Additionally, lens behaviour is also to be tested regarding repeatability of distortion with refocusing as well as its independence from changing focusing distances.

2. CALIBRATION APPROACH

2.1. Lenses and Photography

Two off-the-shelf 17 mm lenses, RMC Tokina 17/3.5 and SP Tamron 17/3.5, were used on a small format Nikon F4 camera. It was decided that, for reasons of simplicity, no test-field would be used and their partial calibration would be performed by means of images of straight lines, in the sense of the well-documented 'plumb-line method' as laid out by Brown (1971); among a variety of other interesting uses (Petsa, 1995), this constitutes a further exploitation of straight lines in photogrammetric tasks. In the general context of medium to low accuracy requirements of many architectural/archaeological tasks, lines found in urban environments were considered, rather than artificial lines, in the step of similar uses of the method with aerial and/or terrestrial cameras (Fryer, 1987; Fryer & Goodin, 1989). Several objects which contain, or form, rectilinear patterns (house façades, ceilings, lattices) were recorded from varying distances (50 cm to infinity). These patterns consisted of vertical and/or horizontal lines; some of them were photographed with both lenses, others only with one of them.

2.2. Measurement of Lines

Paper prints enlarged $\times 4.5$ were produced and scanned at 500 dpi, resulting in a pixel size of $\sim 11 \mu\text{m}$ in negative scale. The lines were digitised manually within a graphics environment. Care was taken to select possibly long lines well distributed over the whole negative frame; evidently, lines close to the edges of the image play a crucial role. Points were sampled with approximately equal frequency, and were subsequently transformed to the image coordinate system defined by the four corners of the frame.

2.3. Mathematical Model

The basic idea here is that, due to lens distortions, rectilinear objects appear on the image as curvilinear. Hence, line-fitting procedures which simultaneously take this fact into account will allow to estimate the distortions. Ignoring the principal point, an image line is best expressed here (according to its slope) in the following alternative forms

$$\begin{aligned} |x_i - x_{i+n}| \leq |y_i - y_{i+n}| &\rightarrow x - \ddot{a}x + t_y(y - \ddot{a}y) + b_x = 0 \\ |x_i - x_{i+n}| > |y_i - y_{i+n}| &\rightarrow t_x(x - \ddot{a}x) + y - \ddot{a}y + b_y = 0 \end{aligned}$$

t_x , t_y being the slopes against the x , y axes, respectively, and b_x , b_y the intercepts with the same axes, while $\ddot{a}x$, $\ddot{a}y$ represent the distortions in x and y . If for radial symmetric lens distortion only the first two polynomial coefficients k_1 , k_2 are used, the two terms $\ddot{a}x$, $\ddot{a}y$ (referred to the center of the image and not to the point of symmetry) become

$$\ddot{a}x_R = x(k_1 r^2 + k_2 r^4) \quad \ddot{a}y_R = y(k_1 r^2 + k_2 r^4)$$

In the line-fitting adjustment, x , y image coordinates are treated as observations. For n lines, the values of $2n + 2$ unknowns are to be estimated. The use of the linearised polynomial for decentering lens distortion (Brown, 1966)

$$\ddot{a}x_D = p_1(r^2 + 2x^2) + 2p_2xy \quad \ddot{a}y_D = p_2(r^2 + 2y^2) + 2p_1xy$$

adds two further unknowns p_1 , p_2 . (Decentering distortion

was practically impossible to grasp with the data used, as will be discussed later.)

2.4. Calibration of the Distortion Curve

Of course, the immediate adjustment result is coefficients describing the radial symmetric distortion curve in an "un-calibrated" form. The coefficients may be directly used to correct image coordinates and subsequently determine a corresponding camera constant; alternatively, they might well be employed in the context of image projective transformation. Nevertheless, it is expedient to bring them to a more familiar (and comparable) "calibrated" form.

Let $\ddot{a}r$ denote the radial symmetric distortion coupled with a camera constant c . A projectively equivalent expression $\ddot{a}r'$ of distortion corresponding to $c' = c + \ddot{a}c$ is obtained as (see also Schøler, 1964):

$$\ddot{a}r' = \left(1 + \frac{\ddot{a}c}{c}\right)\ddot{a}r - \frac{\ddot{a}c}{c}r$$

Among the well-known possible criteria for the calibration of distortion curves, here the defined integral

$$D = \int_0^{r_{\max}} (\ddot{a}r')^2 dr$$

is minimised. The result is a value of $\ddot{a}c/c$, from which the coefficients k_1' , k_2' along with coefficient k_0' of the linear term of the calibrated polynomial are computed.

3. CALIBRATION RESULTS

3.1. Radial Symmetric Lens Distortion

A total of 13 photographs were used for partial calibration (5 for the Tamron lens and 8 for the Tokina lens). Initially, several tests were carried out with both lenses regarding repeatability of resulting distortions from the same photograph under varying conditions. From these, the following general conclusions may be drawn:

- Repeated estimations of distortion based on different numbers of lines (provided that these are well distributed over the frame) seem to give similar results. It is believed that, generally speaking, about 10 lines are sufficient.
- About 15 sampled points per line are considered as fully describing a curved line, resulting (according to line length) in sampling intervals of 1–2 mm in negative scale.
- The use of the first two terms of the distortion polynomial clearly appears as sufficient for expressing distortion (the contribution of term $k_3 r^7$ was found negligible).

Based on these tests, distortion curves for the two lenses were estimated, as shown in Table 2 and Figs. 3 and 4. It is seen in Table 2 that the rms deviations of points from the best-fitting lines (\acute{o}_0) fell radically when the distortion coefficients were introduced as additional unknown parameters (\acute{o}_R). Thus, the mean \acute{o}_0 values for the two lenses are 70 μm and 50 μm , with mean \acute{o}_R falling to 15 μm .

The latter value corresponds to 1.5 pixel in negative scale and is indeed regarded as acceptable within the limits of the adopted calibration approach and the given measuring precision.

Table 2. Line Fitting of Horizontal (H) and Vertical (V) Lines – σ : rms deviations from best-fitting lines in μm –					
		σ_0 Ignoring distortions			
		σ_R With radial distortion			
		σ_{RD} With radial and decentering distortions			
Image	Focus	Lines	σ_0	σ_R	σ_{RD}
<i>RMC Tokina Lens</i>					
1	5 m	1H + 10V	53	15	13
2	5 m	2H + 13V	50	12	10
3	2 m	1H + 8V	62	18	13
4	1 m	12H + 0V	93	14	14
5	2 m	3H + 5V	63	12	11
6	1 m	2H + 11V	60	15	13
7	3 m	0H + 9V	58	21	15
8	3 m	10H + 0V	93	20	10
<i>SP Tamron Lens</i>					
1	∞	6H + 6V	43	16	15
2	∞	6H + 6V	48	11	10
3	∞	6H + 6V	44	13	13
4	∞	6H + 8V	44	15	14
5	2 m	0H + 11V	53	16	14

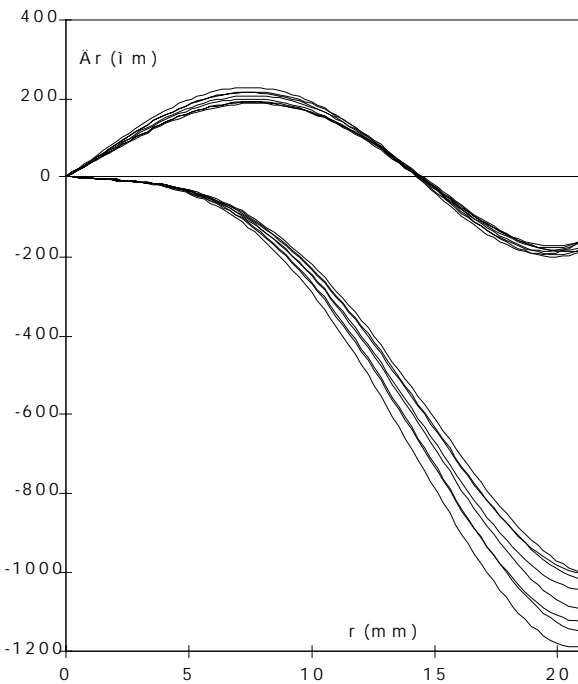


Figure 3. Initial and calibrated radial symmetric distortion curves for the RMC Tokina lens.

As presented in Figs. 3 – 4, distortion curve repeatabilities are good, despite varying conditions regarding direction or number of lines and focusing distance: for both lenses, discrepancies among individual distortion curves did not exceed, in extreme cases, 50 μm . The uncertainty of the curves may also be described by the standard deviations of calibrated distortion values, for every radial distance, calculated from all images. For both lenses used, these were maximally $\pm 20 \mu\text{m}$ at the corners of the negative.

The Tokina lens (see Fig. 3) is characterised by a barrel-type distortion curve which reaches, in its calibrated form, 250 μm at the most. The Tamron lens (see Fig. 4), on the other hand, displays a calibrated distortion pattern of the pin-cushion type, growing to about 350 μm at the corners

of the negative.

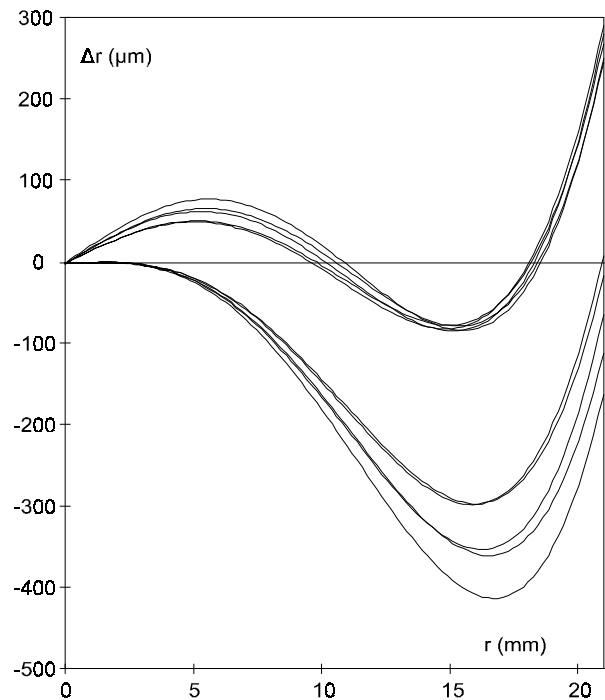


Figure 5. Initial and calibrated radial symmetric distortion curves for the SP Tamron lens.

3.2. Decentering Lens Distortion

As was expected, in view of the small residual deviations of line-fitting (relative to pixel size) when accounting for radial symmetric lens distortions, it has not been possible to reliably (repeatably) estimate decentering distortion. In this sense, the improvement seen in Table 2 is negligible.

3.3. Tests with Relative Orientation

In a further check four stereopairs, two for each lens, of approximately the same scale were taken with convergent axes. These were relatively orientated on the basis of 50 points using the nominal focal length and mean distortion curves interpolated to all data available. Results given in Table 5 illustrate clearly the improvements in the image coordinate residuals. It is noted that this improvement in fact corresponded to a better object reconstruction, which was established by comparing the relative directions of lines in space as reconstructed with both orientations.

Table 5. Precision of Relative Orientations – σ : rms image coordinate residuals in μm –				
		σ_0 Without correction of radial distortion		
		σ_R With correction of radial distortion		
Lens	Tokina	Tokina	Tamron	Tamron
σ_0	30	22	37	47
σ_R	12	9	15	16

3.4. Comparison with a Second Tokina Lens

In order to further check repeatability in the estimation of distortion, two images taken with another Tokina lens of the same type were measured. Keeping the denotations of Table 2, the results are given in Tables 6 and 7.

Image	Focus	Lines	$\hat{\sigma}_O$	$\hat{\sigma}_R$	$\hat{\sigma}_{RD}$
1	∞	5H + 5V	70	15	14
2	∞	7H + 2V	82	15	15

Image	$k_1 \times 10^{-4}$	$k_2 \times 10^{-7}$	$k_0' \times 10^{-2}$	$k_1' \times 10^{-4}$	$k_2' \times 10^{-7}$
1	-2.800	3.961	4.219	-2.918	4.128
2	-2.825	3.835	4.389	-2.949	4.003

These two distortion curves are within the range of those shown in Fig. 3 for the first Tokina lens. This constitutes a strong indication that the behaviour of the particular lens type displays a certain stability.

3.5. Correction of Digital Images

According to the application, the images may or may not have to be pre-corrected; mapping using a digital photogrammetric system with stereoviewing facility constitutes an example for the first case. In such instances, the new images which refer to a lens freed from distortion are produced digitally (Figs. 8–11). As mentioned above, camera constants also have to be determined for these images.

4. CONCLUDING REMARKS

Super-wide-angle lenses used with small format amateur cameras can prove useful in various applications in architecture and archaeology. Using straight lines, their radial symmetric distortion curves have been estimated. These display a satisfactory repeatability, providing strong indications for their photogrammetric potential. Further tests are planned, however, using a test-field and more lenses of the same type for assessing conclusively the expected photogrammetric accuracies.

REFERENCES

- Boulianne, M., Nolette, C., Agnard, J.-P., Brindamour, M., 1997. Hemispherical photographs used for mapping confined spaces. *Photogrammetric Engineering & Remote Sensing*, 63(9):1103-1109.
- Brown, D.C., 1966. Decentering distortion of lenses. *Photogrammetric Engineering*, 32(3):444-462.
- Brown, D.C., 1971. Analytical calibration of close-range cameras. *Photogrammetric Engineering*, 37(8):855-866.
- Fryer, J.G., Goodin, D.J., 1989. In-flight aerial camera calibration from photography of linear features. *Photogrammetric Engineering & Remote Sensing*, 55(12):1751-1754.
- Fryer, J.G., 1987. Innovations in photogrammetry: some student examples. *Australian Surveyor*, 33(7):602-615.
- Petsa, E., 1995. *Line Photogrammetry*. Ph.D. Dissertation, National Technical University of Athens, pp. 248.
- Schöler, H., 1964. Umrechnung von Kammerkonstanten bei wechselnden Abstimmungsbedingungen. *Xth ISP Congress*, Kommission I, Lisbon.

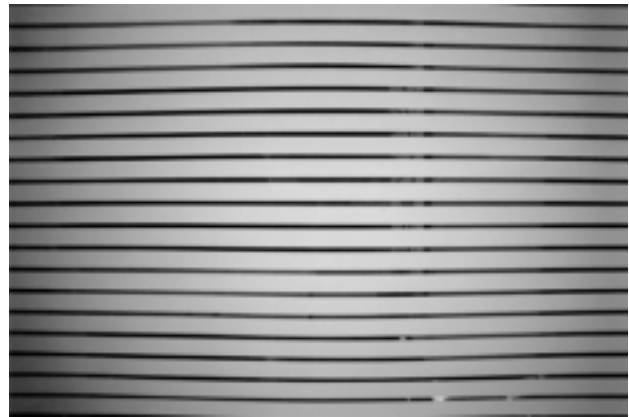


Figure 8. Tokina lens: initial image.



Figure 9. Tokina lens: corrected image.



Figure 10. Tamron lens: initial image.



Figure 11. Tamron lens: corrected image.

